

A Dynamic model for the Lagrangian Averaged Navier-Stokes- Equations

Hongwu Zhao and Kamran Mohseni

Aerospace Engineering Sciences
University of Colorado, 107-81
Boulder, CO 80309-0429
Tel: (303) 492 0286 (Mohseni)
Fax: (303) 492 7881
Email: mohseni@colorado.edu

April 17, 2024

Abstract

A dynamic procedure for the Lagrangian Averaged Navier-Stokes- (LANS-) equations is developed where the variation in the parameter ϵ in the direction of anisotropy is determined in a self-consistent way from data contained in the simulation itself. In order to derive this model, the incompressible Navier-Stokes equations are Helmholtz-filtered at the grid and a test filter levels. A Germano type identity is derived by comparing the filtered subgrid scale stress terms with those given in the LANS- equations. Assuming constant ϵ in homogeneous directions of the flow and averaging in these directions, results in a nonlinear equation for the parameter ϵ , which determines the variation of ϵ in the non-homogeneous directions or in time. Consequently, the parameter ϵ is calculated during the simulation instead of a pre-defined value. The dynamic model is initially tested in forced and decaying isotropic turbulent flows where ϵ is constant in space but it is allowed to vary in time. It is observed that by using the dynamic LANS- procedure a more accurate simulation of the isotropic homogeneous turbulence is achieved. The energy spectra and the total kinetic energy decay are captured more accurately as compared with the LANS- simulations using a fixed ϵ . In order to evaluate the applicability of the dynamic LANS- model in anisotropic turbulence, a priori test of a turbulent channel flow is performed. It is found that the parameter ϵ changes in the wall normal direction. Near a solid wall, the length scale ϵ is seen to depend on the distance from the wall with a vanishing value at the wall. On the other hand, away from the wall, where the turbulence is more isotropic, ϵ approaches an almost constant value. Furthermore, the behavior of the subgrid scale stresses in the near wall region is captured accurately by the dynamic LANS- model. The dynamic LANS- model has the potential to extend the applicability of the LANS- equations to more complicated anisotropic flows.

1 Introduction

Turbulent flows play an important role in many areas of engineering fluid mechanics as well as atmospheric and oceanic flows. A accurate simulation of a turbulent flow requires that the energetics of the large scale energy containing eddies, dissipative small scales, and inter-scale interactions to be accounted for. In direct numerical simulations (DNS) all the involved scales are directly calculated. DNS is believed to provide the most comprehensive representation of the governing equations of fluid flows; the so-called Navier-Stokes (NS) equations. Owing to the very high Reynolds numbers encountered in most problems of interest, the disparity between the large scales and small scales, which represents the computational size of the problem, rapidly grows with the Reynolds number. Consequently, DNS can resolve only a small fraction of the turbulent activity for high Reynolds number flows.

While the direct numerical simulation of most engineering flows seems unlikely in near future, turbulence modeling could provide qualitative and in some cases quantitative measures for many applications. Large Eddy Simulations (LES) and the Reynolds Averaged Navier-Stokes Equations (RANS) are among the numerical techniques to reduce the computational intensity of turbulent calculations. In LES, the dynamics of the large turbulence length scales are simulated accurately and the small scales are modeled. The vast majority of contemporary LES make use of eddy-viscosity based Subgrid-Scale (SGS) models in conjunction with the spatially-averaged (filtered) Navier-Stokes Equations. In this approach, the effect of the unresolved turbulence is modeled as an effective increase in the molecular viscosity. On the other hand, RANS models are obtained by time averaging the Navier-Stokes equations. In this case most of the unsteadiness is averaged out. Consequently, the time mean quantities are calculated while the faster scale dynamics are modeled. RANS simulations are often more affordable than LES, however, their accuracy is somewhat limited in many applications [24].

More recently, Holm, Marsden and their coworkers [12] introduced a Lagrangian averaging technique for the mean motion of ideal incompressible flows. Figure 1 contrasts the derivation of LES, RANS, and the Lagrangian Averaged Navier-Stokes- (LANS-) equations. Unlike the traditional averaging or filtering approach used for both RANS and LES, where the Navier-Stokes equations are averaged or spatially filtered, the Lagrangian averaging approach is based on averaging at the level of the variational principle. In the isotropic Lagrangian Averaged Euler- (LAE-) equations, fluctuations smaller than a specified scale are averaged at the level of the flow maps [3]. Mean fluid dynamics are derived by applying an averaging procedure to the action principle of the Euler equations. As shown in Figure 1, both the Euler and the Navier-Stokes equations can be derived in this manner (see Marsden & Ratiu [18] for a variational derivation of the Euler equations). The usual Reynolds Averaged Navier-Stokes (RANS) or LES equations are then obtained through the subsequent application of either a temporal or spatial average. The critical difference with the Lagrangian averaging procedure is that the Lagrangian (kinetic energy minus potential energy) is averaged prior to the application of Hamilton principle and a closure assumption is applied at this stage. This procedure results in either the Lagrangian averaged Euler Equations (LAE-)¹ or the Lagrangian averaged Navier-Stokes Equations (LANS-), depending on whether or not a random walk component is added in order to produce a true molecular diffusion term. Since the Hamilton principle is applied after the Lagrangian averaging is performed, all the geometrical properties (e.g. invariants) of the inviscid dynamics are retained even in the presence of the model terms which arise

¹ In this nomenclature, Δ is used to denote the filtering scale (i.e. the simulation faithfully represents motions on a scale larger than Δ).

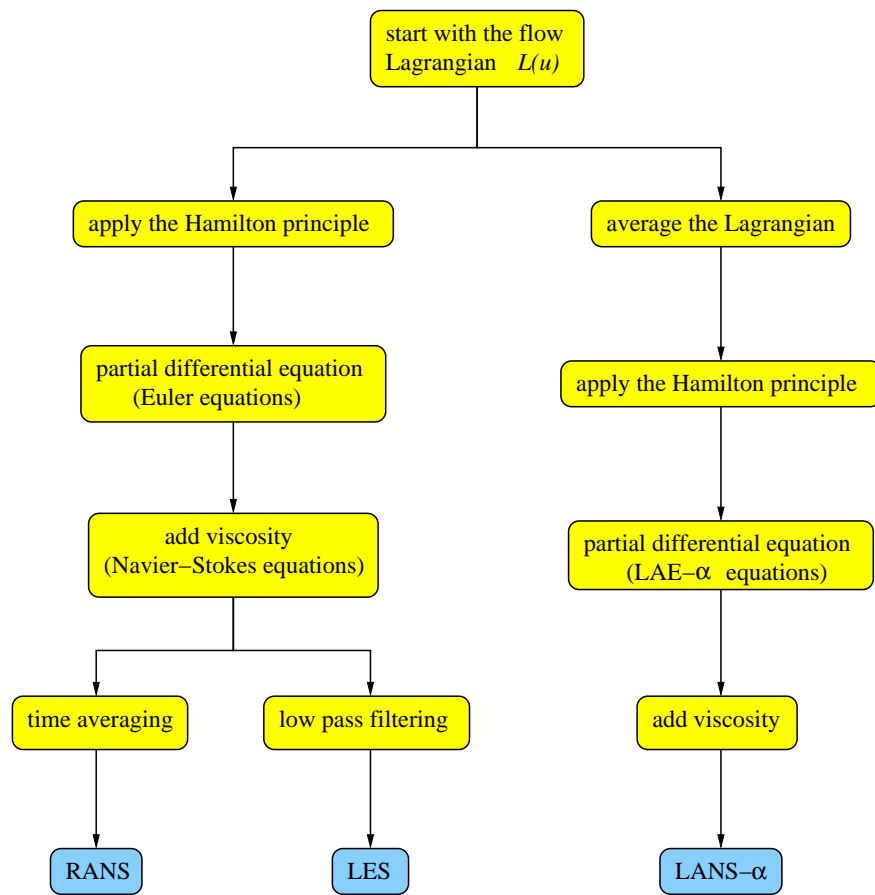


Figure 1: Derivation of the averaged flow equations.

from the closure assumption [12; 11; 10]. For instance, LAE equations possess a Kelvin circulation theorem. Thus it is potentially possible to model the transfer of energy to the unresolved scales without an incorrect attenuation of quantities such as resolved circulation. This is an important distinction from any engineering and geophysical flows where the accurate prediction of circulation is highly desirable.

Numerical simulations by Chen et al [5] and Mohseni et al [22] showed the capability of the LANS- equations in simulating isotropic homogeneous turbulence. However, most engineering and geophysical flows of interest are often anisotropic. For example, due to rapid damping of turbulent fluctuations in the vicinity of a wall, the application of the isotropic LANS- equations with a constant ν is not appropriate for long term calculations. In order to capture the correct behavior in such systems the parameter ν must be spatially or/and temporally varied in the direction of anisotropy [4], i.e. wall normal direction. There has been some attempt (with limited success) in order to remedy this problem. A successful dynamic LANS- model is yet to be formulated and tested. There are at least two approaches to anisotropy in the LANS- equations:

- (i) To derive a set of anisotropic LANS- equations. See alternative derivations in [10; 19].
- (ii) Use the isotropic LANS- equations, but with a variable ν to compensate for the anisotropy.

At this point much more work must be done on the anisotropic LANS- equations before they can be applied to practical problems. The second approach listed above is what will be explored in this study.

This paper is organized as follows: The isotropic LANS- equations and some of their main features are summarized in section 2. A dynamic LANS- approach is proposed in section 3 where the variation in the parameter ν in the direction of anisotropy is determined in a self-consistent way from the data contained in the simulation itself. Our approach will be developed in the same spirit as the dynamic modeling procedure for conventional LES [8; 9; 20; 13] which has achieved widespread use as very effective means of estimating model parameters as a function of space and time as the simulation progresses. The incompressible Navier-Stokes equations are Helmholtz- filtered at the grid and a test filter levels. A Germano type identity is derived by comparing the filtered subgrid scale stress terms with those given in the LANS- equations. Considering a constant value of ν and averaging in the homogeneous directions of the flow results in a nonlinear equation for the parameter ν , which determines the variation of ν in the non-homogeneous directions or time. This nonlinear equation is solved by an iterative technique. Consequently, the parameter ν is calculated during the simulation instead of a fixed and pre-defined value.

Numerical techniques for simulating the dynamic LANS- model in this study are described in section 4. The performance of the dynamic LANS- model in simulating forced and decaying isotropic homogeneous turbulent flows are considered in section 5. In statistically equilibrated forced turbulence, the parameter ν should remain constant in time and space. In decaying isotropic turbulence, the parameter ν could change in time as the integral scales of the turbulent flow changes. In order to demonstrate the applicability of the dynamic LANS- model of this study in anisotropic flows, a priori test of turbulent channel flows are also performed in section 5. Concluding results are presented in section 6.

2 The Isotropic LANS- Equations

The incompressible isotropic LANS- equations for the large scale velocity u are given by (see [12] for a derivation)

$$\frac{\partial u}{\partial t} + (u \cdot \nabla) u = -\nabla p + \frac{1}{Re} \nabla^2 u + \nabla \cdot \tau(u); \quad (1)$$

$$\nabla \cdot u = 0; \quad (2)$$

where $\tau(u)$ is the subgrid stress tensor defined as [3]

$$\tau(u) = \frac{1}{2} (1 - \Delta^2)^{-1} (\nabla u \cdot \nabla u^T + \nabla u^T \cdot \nabla u - \nabla^2 u \cdot \nabla u + \nabla^2 u^T \cdot \nabla u); \quad (3)$$

The subgrid scale stress $\tau(u)$ is in fact the momentum flux of the large scales caused by the action of smaller, unresolved scales. Here ℓ is a constant length scale introduced during the averaging process. Note that for vanishing parameter ℓ the NS equations will be recovered.

The LANS- equations can be represented equivalently by

$$\frac{\partial v}{\partial t} + (u \cdot \nabla) v + \nabla \cdot (u \otimes u) = -\nabla P + \frac{1}{Re} \nabla^2 v; \quad \text{where } v_i \text{ is defined as } v = u - \ell^2 \Delta u; \quad (4)$$

The modified pressure P in these equations is determined, as usual, from the incompressibility condition: $\nabla \cdot u = 0$ and $\nabla \cdot v = 0$.

One interpretation for the equations (1) is that they are obtained by averaging the Euler equations in Lagrangian representation over rapid fluctuations whose scale are of order ℓ . In this respect, one can show that the Lagrangian averaged Euler equations can be regarded as geodesic equations for the H^{-1} metric on the volume preserving diffeomorphism group, as Arnold [2] did with the L_2 metric for the Euler equations. Note that in calculating the SGS stress $\tau(u)$ in equation (3) one needs to calculate the inverse of the Helmholtz operator $(1 - \ell^2 \Delta)^{-1}$, which implies the need to solve a Poisson equation. While efficient numerical treatment of the Poisson equation, or its possible elimination through rational approximation will be a focus of a future publication, we note, in passing, that the inverse of the Helmholtz operator can be expanded in ℓ^2 to higher orders of the Laplacian operator as shown in below

$$(1 - \ell^2 \Delta)^{-1} = 1 + \ell^2 \Delta + \frac{1}{2} \ell^4 \Delta^2 + \dots;$$

Consequently, solving a Poisson equation for inverting the Helmholtz operator could be avoided.

It is interesting to note that the Lagrangian averaging technique preserves the Hamiltonian structure of the governing equations in the inviscid limit while the effects of small scales on the macroscopic features of large scale are taken into account in a conservative manner. The Hamiltonian and Lagrangian formulations of ideal fluids are both basic and useful. These formulations are part of a more general framework of geometric mechanics, which plays a vital role in the development of new continuum models suited for computation, as well as numerical algorithms that preserve structure at the discrete level. In recent years the geometric approach to fluid mechanics has been quite successful. Geometrical methods provide a framework for the study of nonlinear stability [1], variational integrators [14; 16], statistical equilibrium theory [6; 21], and many other interesting topics in fluid dynamics. The Lagrangian averaged Navier-Stokes- uses ideas from geometric mechanics and offers a theoretically and computationally attractive approach to the turbulence closure problem.

3 Derivation of a Dynamic LANS-Model

The LANS- equations for the large scale velocity u are given by equations (1), where τ is the subgrid stress tensor defined in (3). This set of equations for u is similar to the grid filtered equation in the dynamic LES. In analogy with the dynamic LES one can obtain an equation for the filtering length scale, Δ , by filtering the Navier-Stokes equations

$$\frac{\partial u_i}{\partial t} + u_j \frac{\partial u_i}{\partial x_j} = -\frac{\partial p}{\partial x_i} + \frac{1}{Re} \frac{\partial^2 u_i}{\partial x_j \partial x_j}; \quad (5)$$

with the Helmholtz related filters

$$u = (1 - \Delta^2)^{-1} u; \quad \text{grid filter}; \quad (6)$$

$$\hat{u} = (1 - b^2)^{-1} (1 - \Delta^2)^{-1} u; \quad \text{test filter}; \quad (7)$$

to obtain

$$\frac{\partial u_i}{\partial t} + \frac{\partial u_i u_j}{\partial x_j} = -\frac{\partial p}{\partial x_i} + \frac{1}{Re} \frac{\partial^2 u_i}{\partial x_j \partial x_j} - \frac{\partial \tau_{ij}}{\partial x_j}; \quad (8)$$

$$\frac{\partial \hat{u}_i}{\partial t} + \frac{\partial \hat{u}_i \hat{u}_j}{\partial x_j} = -\frac{\partial \hat{p}}{\partial x_i} + \frac{1}{Re} \frac{\partial^2 \hat{u}_i}{\partial x_j \partial x_j} - \frac{\partial T_{ij}}{\partial x_j}; \quad (9)$$

where

$$\tau_{ij} = \overline{u_i u_j} - u_i u_j;$$

$$T_{ij} = \overline{\hat{u}_i \hat{u}_j} - \hat{u}_i \hat{u}_j;$$

Using an idea similar to Germano identity [8], we define

$$L_{ij} = T_{ij} - \Delta^2 \tau_{ij} = \overline{\hat{u}_i \hat{u}_j} - \hat{u}_i \hat{u}_j; \quad (10)$$

where the subgrid scale stresses under two filtering actions can be modeled by the LANS- subgrid term in equation (3). Therefore,

$$\tau_{ij} = \Delta^2 (1 - \Delta^2)^{-1} M_{ij}; \quad (11)$$

$$T_{ij} = \Delta^2 (1 - \Delta^2)^{-1} N_{ij}; \quad (12)$$

where

$$M_{ij} = \frac{\partial u_i}{\partial x_k} \frac{\partial u_j}{\partial x_k} - \frac{\partial u_k}{\partial x_i} \frac{\partial u_k}{\partial x_j} + \frac{\partial u_i}{\partial x_k} \frac{\partial u_k}{\partial x_j} + \frac{\partial u_j}{\partial x_k} \frac{\partial u_k}{\partial x_i};$$

$$N_{ij} = \frac{\partial \hat{u}_i}{\partial x_k} \frac{\partial \hat{u}_j}{\partial x_k} - \frac{\partial \hat{u}_k}{\partial x_i} \frac{\partial \hat{u}_k}{\partial x_j} + \frac{\partial \hat{u}_i}{\partial x_k} \frac{\partial \hat{u}_k}{\partial x_j} + \frac{\partial \hat{u}_j}{\partial x_k} \frac{\partial \hat{u}_k}{\partial x_i};$$

Combining equations (10)-(12), one obtains

$$L_{ij} = \Delta^2 (1 - \Delta^2)^{-1} N_{ij} - \Delta^2 (1 - \Delta^2)^{-1} (1 - \Delta^2)^{-1} M_{ij}; \quad (13)$$

or

$$L_{ij} = \tau^2 (\tau^2 \hat{N}_{ij} - \hat{M}_{ij}); \quad (14)$$

where $\tau = \Delta_t / \Delta x$. Multiplying both sides of the above equation by S_{ij} , to yield

$$L_{ij} S_{ij} = \tau^2 (\tau^2 \hat{N}_{ij} - \hat{M}_{ij}) S_{ij}; \quad (15)$$

Taking spatial averaging of both sides of the above equation in homogenous directions, one obtains

$$\tau^2 = \frac{\langle L_{ij} S_{ij} \rangle}{\langle \tau^2 \hat{N}_{ij} - \hat{M}_{ij} \rangle S_{ij}}; \quad (16)$$

where

$$S_{ij} = \frac{1}{2} \left(\frac{\partial u_i}{\partial x_j} + \frac{\partial u_j}{\partial x_i} \right);$$

The denominator in equation (16) could approach zero, where it creates a singularity. In dynamic LES, Lilly [17] used a least square approach to eliminate the singularity in Germano's model. By a similar least square approach a nonlinear equation for τ^2 could be found as

$$\tau^2 = F(\tau^2) = \frac{\langle L_{ij} (\tau^2 \hat{N}_{ij} - \hat{M}_{ij}) \rangle}{\langle \tau^2 \hat{N}_{ij} - \hat{M}_{ij} \rangle \langle \tau^2 \hat{N}_{ij} - \hat{M}_{ij} \rangle}; \quad (17)$$

which does not have the singularity problem as in equation (16). This is a nonlinear equation for τ^2 . All the quantities in equation (17) can be calculated during a LANS- simulation. Therefore, equation (17) provides a nonlinear equation for dynamically calculating the value of τ^2 during the simulation.

At this point the potential values for the free parameter τ are required. Writing the grid and test filters in equations (6) and (7) in the Fourier space, one obtains

$$u = \frac{u}{1 + \tau^2 k^2}; \quad (18)$$

and

$$\hat{u} = \frac{u}{(1 + \tau^2 k^2)(1 + \tilde{\tau}^2 k^2)} = \frac{u}{1 + (\tau^2 + 1) \tilde{\tau}^2 k^2} = \frac{u}{1 + \tilde{\tau}^2 k^2} \quad \text{as } k \rightarrow 1; \quad (19)$$

where $(\tilde{\tau})$ stands for variables in the Fourier space, k is the wavenumber, and $\tilde{\tau}$ corresponds to filter scale for the test filter. Since $\tilde{\tau} = \frac{\tau}{1 + \tau^2}$, one can realize that as long as $\tau > 0$, the test filter have a larger filter scale than the grid filter. Figure 2 shows the relative positions of the grid filter scale and the test filter scale $\tilde{\tau}$ on a schematic of the energy spectrum for a high Reynolds number flow. In order to accurately model the subgrid scale stress, both the grid filter and the test filter scales must be located in the inertial sub-range of the energy spectrum. It should be pointed out that the iterative calculation required in equation (17) does not require new flow field calculations, and the iteration at each time step is carried out using the existing flow field at the same time step. Similar to the dynamic LES model, the present dynamic LANS- model has a free parameter τ , which is related to the characteristic length scale of the grid and test filters.

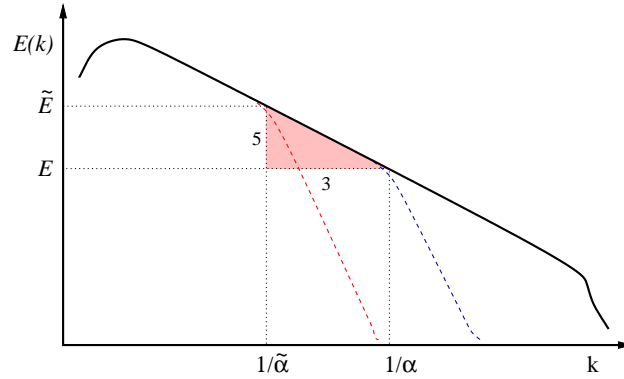


Figure 2: The positions of grid and test filter scales on the turbulent kinetic energy spectrum .

The dynamic model given in equation (17) is designed to capture the length scale variations in space and time. Aside from the isotropic homogeneous turbulent flows, it is well suited for anisotropic flows such as wall bounded turbulence or mixing flow turbulence, where the turbulence length scales could change in space or in time. In cases where there are directions of homogeneity, such as the streamwise and spanwise direction in a channel flow, one can average the parameter over the homogeneous directions. In a more general situation, we expect to replace the plane average, used in the channel flow, by an appropriate local spatial or time averaging scheme. For isotropic homogeneous turbulence, α is regarded as a constant in space and changes only in time.

4 Numerical Method

The dynamic procedure in this study is initially tested for forced and decaying isotropic turbulence where the parameter α is constant over the computational domain, but can vary in time. Furthermore, a priori test of the dynamic LANS- σ procedure in a turbulent channel flow is investigated. In this section the numerical technique for solving the governing equations are summarized.

Isotropic homogeneous turbulence. The computations are performed in a periodic cubic box of side 2π . A standard parallel pseudospectral scheme with periodic boundary conditions are employed. The spatial derivatives are calculated in the Fourier domain, while the nonlinear convective terms are computed in the physical space. A fourth order Runge-Kutta scheme is implemented to advance the flow field in time. The two third rule is used in order to eliminate the aliasing errors. Therefore, the upper one third of the wave modes are discarded at each stage of the Runge-Kutta scheme. The initial velocity field for each case was divergence free and constructed to generate an energy spectrum of the form

$$E(k) = k^4 \exp[-2(k/k_p)^2]:$$

The value of k_p corresponds to the peak in the energy spectrum. The initial pressure fluctuations were obtained from the solution of a Poisson equation.

Turbulent flow in a channel. DNS data from deAlamio and J. Jimenez [7] are employed for the a priori test. The computational domain in this case, normalized based on the half channel

height, is spanned 8 in the streamwise and 4 in the spanwise directions. The spatial derivatives are calculated by the pseudospectral method in streamwise and spanwise directions and by the Chebychev-tau technique in the wall normal direction. Similar computational techniques have successfully been used for the DNS of channel flows by Kim et al [15] and Moser et al [23]. Grid and test filters of Helmholtz types are applied in both streamwise and spanwise directions, while no explicit filters are applied in the wall normal direction. ν is assumed to be constant in the homogeneous directions, i.e. the streamwise and spanwise directions, in order to solve the nonlinear equations (16) or (17). These equations are solved by an iterative technique. Since both the mean flow and the flow perturbations vanish at the wall, singular behavior might occur in these equations. This can be easily fixed by starting the a priori test a few grid points away from the wall. In actual simulation of the dynamic LANS- equations, one can explicitly put ν to zero below in the immediate vicinity of a wall when the value of ν drops below a threshold. The converged values at each point is used as an initial value for the iteration at the next grid layer.

5 Results and Discussions

Capabilities of the dynamic LANS- model of the previous sections are examined in both isotropic and anisotropic turbulent flows. In isotropic homogeneous turbulence the parameter ν is constant in space but allowed to vary in time. Results of the dynamic model is compared with the isotropic LANS- simulations with a constant ν and with the DNS data.

Decaying isotropic homogeneous turbulence simulations. DNS of a decaying isotropic homogeneous turbulence with initial Taylor Reynolds number of $Re = 72$ (corresponding to a computational Reynolds number $Re = 300$) is performed to be used as a test case. The initial energy spectrum is peaked at $k_p = 4$. The isotropic LANS- and the dynamic LANS- simulations are calculated for both 64^3 (corresponds to 48^3 after dealiasing) and 48^3 (corresponds to 32^3 after dealiasing) resolutions, and direct numerical simulations are performed for 128^3 (corresponds to 85^3 after dealiasing). The eddy turn over time for this case is found to be $\tau = 0.9$. Figure 3 shows the time evolution of ν for $\nu = 0.8; 0.9; 1$; and 1.2 . The values of ν experience a sharp decrease from its initial value during the first eddy turn over time. However, it quickly settle down toward a much slower varying value. Slight changes in ν value after the first eddy turn over time could be traced back to attening of the energy spectrum as the turbulence decays.

The energy spectra at two different times are shown in Figure 4, and the total kinetic energy decay are shown in Figure 5. While a slight dependency on the value of ν is observed, in general, the energy spectrum at various times and the total kinetic energy decay are captured nicely. Mohseni et al [22] demonstrated that in order to accurately simulate a turbulent flow with the LANS- equations, the value of ν should be somewhere, perhaps one decade lower than the peak of the energy spectra toward the grid resolution. Careful considerations of Figures 3 and 4 reveal that the dynamic LANS- model of this study satisfies this criteria for all ν values. In general, one expects that the value of ν to be in the inertial range of the energy spectra in order to correctly capture the dynamics of the large scales. As illustrated in Figures 4 and 5, it is evident that the dynamic LANS- model provides a better estimate of the total kinetic energy decay and the energy spectra over similar simulations with fixed ν calculations.

Forced isotropic homogeneous turbulence simulations. Forced isotropic turbulence is one of the most idealized and extensively simulated turbulent flows. The numerical forcing of a tur-

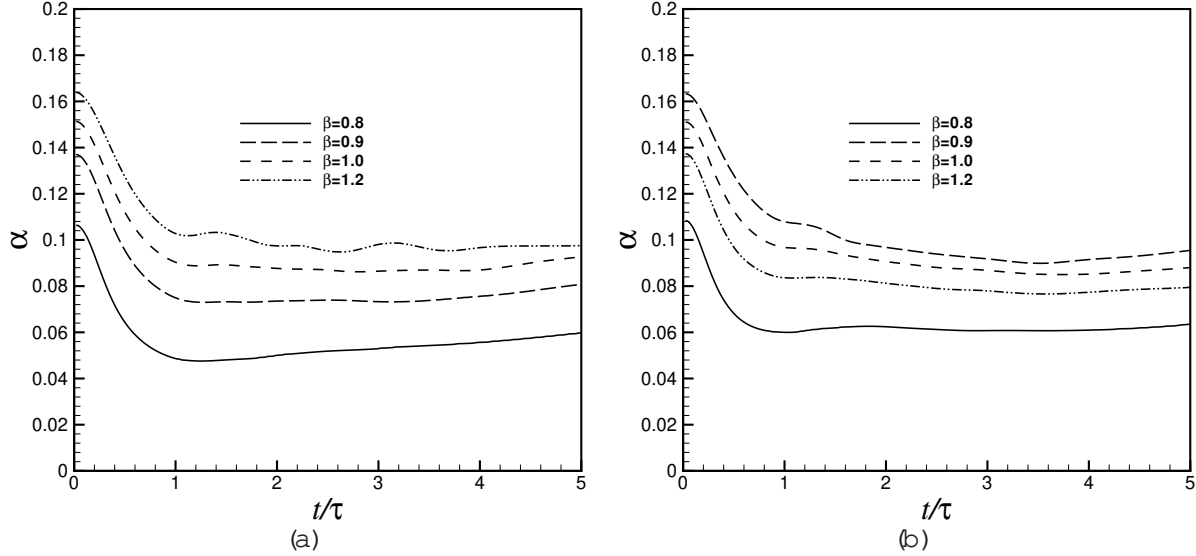


Figure 3: Evolution of α for different β for a decaying isotropic turbulence at $Re = 72$ and $\beta = 0.9$. Grid resolution (a) 48^3 , (b) 32^3 .

bulent flow is usually referred to the artificial addition of energy at the large scales in a numerical simulation. Statistical equilibrium is signified by the balance between the input of kinetic energy through the forcing and its output through the viscous dissipation. In this study, we adopted a forcing method used in Chen et al [5] and Mosheniet al [22] where the wave modes in a spherical shell $k_j = k_0$ of certain width are forced in such a way that the forcing spectrum follows the Kolmogorov $k^{-5/3}$ scaling law, that is

$$f_i = \frac{1}{N} \sum_k \frac{u_i}{u_k u_k} k^{-5/3} : \quad (20)$$

Here f_i and u_i are Fourier transforms of the forcing vector f_i and velocity u_i , N is the number of forced wave modes, and β controls the injection rate of energy at the large scales. This particular forcing technique enforces the energy cascade in the inertial range starting from the first wave mode. In this simulations we choose $k_0 = 2$ and $\beta_0 = 0.1$. The initial Taylor Reynolds number is $Re = 415$ and the initial energy spectrum is peaked at $k_p = 1$, while the eddy turnover time is found to be $\tau = 3.8$. The grid resolution for simulations using the dynamic LANS- equations and the LANS- equations with fixed β is 64^3 , while the DNS data is performed at a grid resolution of 128^3 before dealiasing.

Figure 6 shows the evolution of α for $\beta = 0.8$ and 1.0 . Similar to the decaying turbulence, a sharp decrease in the value of α is observed over the first eddy turnover time, where the values of α settles down toward a constant value. This corresponds to an statistically equilibrated state. As expected, the final value of α is in the inertial range of the energy spectrum.

Figure 7 shows the energy spectrum at $t = 5.8$ for $\beta = 0.8$ and 1.0 . An inertial subrange with $k^{-5/3}$ energy spectrum is evident in the dynamic LANS- simulations. The results of the dynamic LANS- simulations are compared with the DNS and the LANS- simulations with $\beta = 0.2$. The energy spectra of the dynamic LANS- simulations for $\beta = 0.8$ and 1.0 show a better agreement with the DNS data than the energy spectra for a LANS- simulation with a constant β .

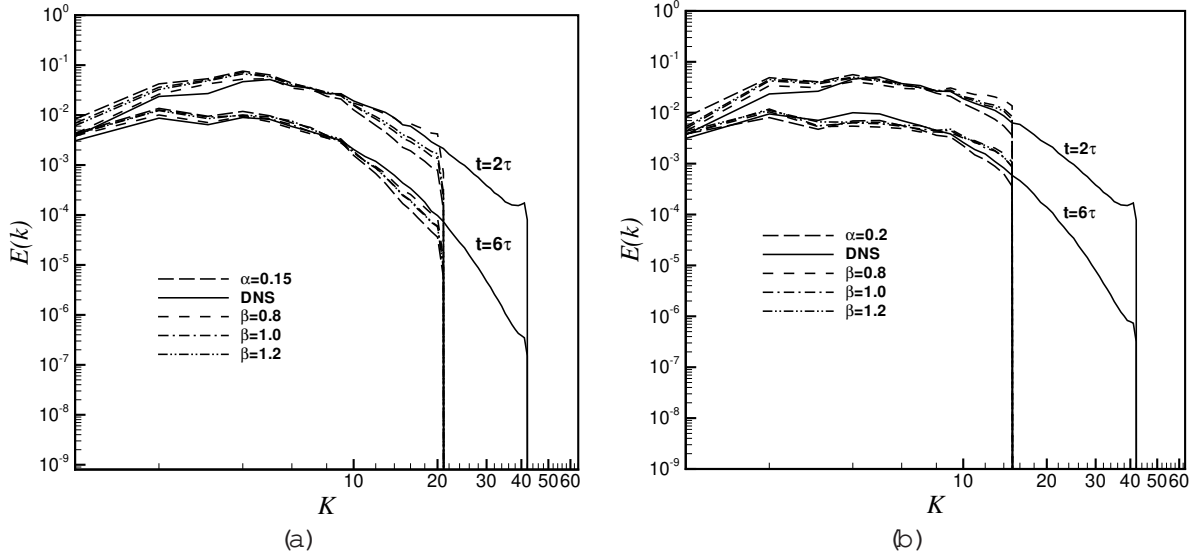


Figure 4: Energy spectra of the DNS, dynamic LANS- β , and LANS- β with fixed α simulations of a decaying isotropic turbulence at $Re = 72$ and $\beta = 0.9$. Grid resolution (a) 48^3 , (b) 32^3 .

A priori test of a turbulent channel flow. A priori test of the dynamic LANS- β model is carried out in order to determine the accuracy of the model in predicting the SGS stresses and the energy dissipation rates in a wall bounded flow. The tests are performed on a DNS data of deLamoro and Jimenez [7] for a turbulent channel flow. The turbulence Reynolds number, based on the wall friction velocity, is $Re = 550$ and the computational grid is $1536 \times 257 \times 1536$ in the streamwise, wall normal, and spanwise directions, respectively. After dealiasing the physically relevant part of the computational domain reduces to $1024 \times 257 \times 1023$. The mean velocity profile, non-dimensionalized by the wall-shear velocity, is depicted in Figure 8(a), where a log layer from $y^+ = 80$ to 220 is observed. Figure 8(b) shows the turbulence intensity profiles from the wall to the middle of the channel in global coordinate which is normalized by half channel height. Maximum turbulence intensities in all directions are located in the wall layer.

Figure 9 shows the variation of β with the distance from the wall in both global and wall coordinates for $\alpha = 0.8; 1.0$; and 1.2 . As demonstrated in Figure 9(b), β values experience a sharp increase in the vicinity of the wall up to $y^+ = 100$. This region of sharp increase in the value of β contains both the viscous sublayer and the buffer layer. Diminishing values of β is observed as one approaches the wall. This is consistent with theoretical expectations that the NS equations ought to be recovered in the laminar layer at the wall. The profile of β in the vicinity of the wall shows minimal dependency on α . Away from the wall and beyond $y^+ = 100$, β shows little variation across the channel. One can argue that the dynamic LANS- β equations in this case divides the flow into two distinct regions: a near wall region that includes both the viscous sublayer and the buffer layer where β is a function of the distance from the wall, and a constant β region which includes the log layer and the outer layer. In the near wall region β keeps an almost log relation with the distance from the wall in wall units. In summary, one can argue that in wall bounded flows, the isotropic LANS- β calculations could be used with a constant β beyond $y^+ = 100$ and with a logarithmic relation in the near region. This projection requires further investigation in LANS- β calculations.

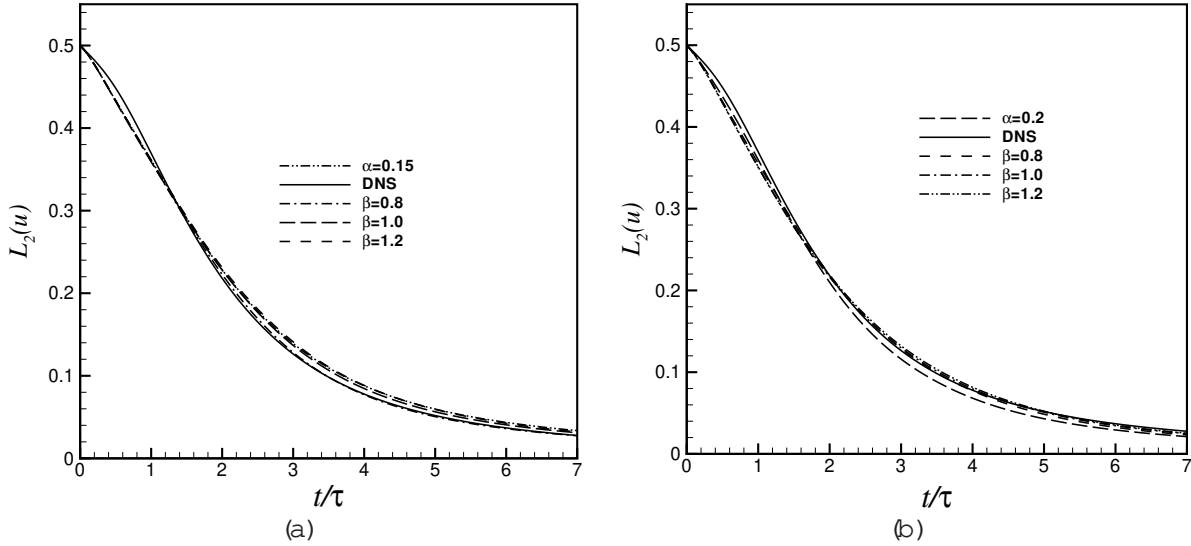


Figure 5: Total kinetic energy decay of the DNS, dynamic LANS- β , and LANS- β with fixed simulations of a decaying isotropic turbulence at $Re = 72$ and $\beta = 0.9$. Grid resolution (a) 48^3 , (b) 32^3 .

Similar to the dynamic LES, one expects that the accuracy of the dynamic LANS- β model to depend on its capability of accurately modeling the subgrid scale stresses. The modeled and the exact SGS stresses in this flow are shown in Figure 10 for the isotropic component $\langle \tau_{11} \rangle$ and Figure 11 for the shear stress component $\langle \tau_{12} \rangle$, where $\langle \cdot \rangle$ stands for averaging in streamwise and spanwise directions. The general trend of the SGS stresses are captured in the dynamic LANS- β model without any ad hoc damping function. Good agreement between the modeled and the exact SGS stresses in the near wall region are observed. The SGS stresses vanish at the wall and in the middle of the channel with a maximum value within the wall layer. The exact and modeled dissipation $\langle \epsilon \rangle$ are compared in Figure 12. Both the SGS stresses and the modeled dissipations are effectively insensitive to variation in β .

6 Conclusions

A dynamic LANS- β model is proposed where the variation in the parameter β in the direction of anisotropy is determined in a self-consistent way from data contained in the simulation itself. The model results in a nonlinear equation for β . Numerical experiments for decaying and forced homogeneous isotropic turbulence are performed using the dynamic LANS- β model. The simulation results in both cases show an improvement over the LANS- β simulations with a fixed β .

A priori test of the dynamic LANS- β model in a channel flow is carried out, where good agreement between the dynamic LANS- β predictions and the DNS data is observed. The parameter β is found to rapidly change in the wall normal direction in the vicinity of the wall. Near the solid wall, the length scale β shows a logarithmic dependence on the wall normal direction in wall units. Away from the wall, and in the middle of the channel, β approaches an essentially constant value. As a result, the turbulent flow is divided into two regions: a constant β region away from the

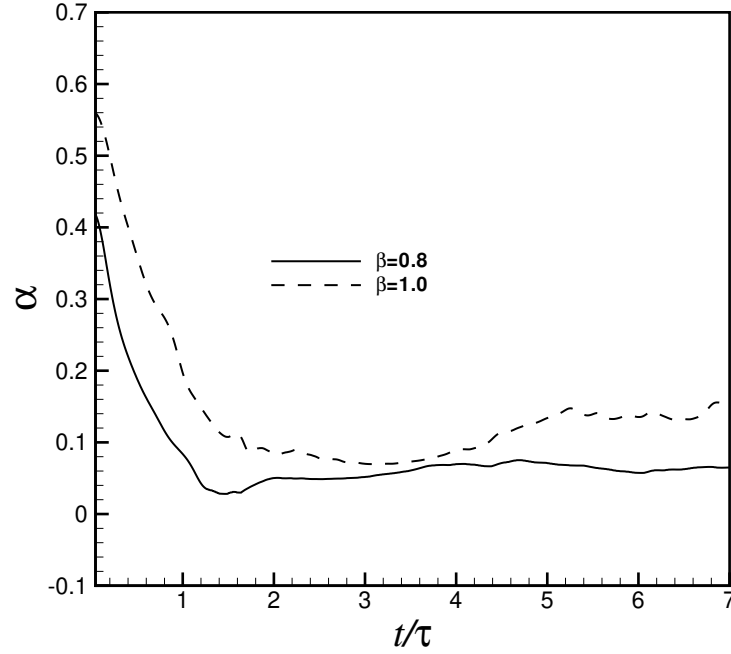


Figure 6: Evolution of α for different β in the forced turbulence case with $Re = 415$ and $\gamma = 3.8$.

wall and a near wall region. In the near wall region, α keeps an almost logarithmic relation with the distance from the wall. Consequently, one can argue that in wall bounded flows, the isotropic LANS- calculations could be used with a constant β beyond $y^+ = 100$ and with a logarithmic relation in the near region. These results indicates a promising application of the dynamic LANS-model in wall bounded turbulent flow simulations.

7 Acknowledgement

The research in this paper was partially supported by the AFOSR contract F49620-02-1-0176. The authors would like to thank B. Kosovic for his initial help in the derivation of the dynamic model and T. Lund for helpful discussions. The DNS data of the channel flow was generously provided by R. Moser and J. Jimenez.

References

- [1] H. Abarbanel, D. Holm, J.E. Marsden, and T. Ratiu. Nonlinear stability of stratified flow. Phys. Rev. Lett., 52:2352{2355, 1984.
- [2] V.I. Arnold. Sur la geometrie differentielle des groupes de Lie de dimension infinie et ses applications a l'hydrodynamique des fluides parfaits. Ann. Inst. Fourier, 16:319{361, 1966.
- [3] H.S. Bhat, R.C. Fetecau, J.E. Marsden, K. Mohseni, and M. West. Lagrangian averaging for compressible fluids. to appear in the SIAM Journal on Multiscale Modeling and Simulation, 2003. Also <http://arxiv.org/abs/physics/0311086>.

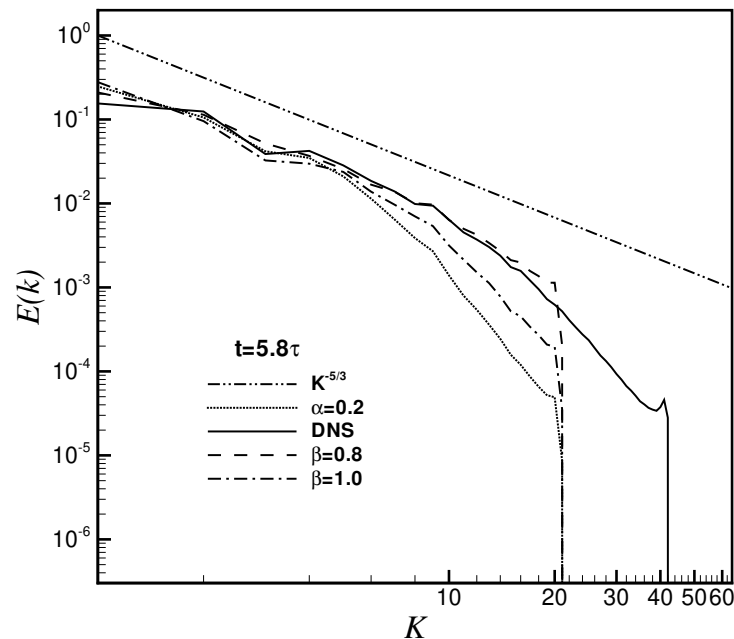


Figure 7: Energy spectra at $t = 5.8\tau$ for the DNS, dynamic LANS- and LANS- with fixed simulations of a forced isotropic turbulence with $Re = 415$ and $\beta = 3.8$.

- [4] S.Y. Chen, C. Foias, D.D. Holm, E. Olson, E.S. Titi, and S. Wynne. Camassa-Holm equations as a closure model for turbulent channel and pipe flow. *Phys. Rev. Lett.*, 81:5338{5341, 1998.
- [5] S.Y. Chen, D.D. Holm, L.G. Margolin, and R. Zhang. Direct numerical simulations of the Navier-Stokes-alpha model. *Physica D*, 133:66{83, 1999.
- [6] A.J. Chorin and J.E. Marsden. *A Mathematical Introduction to Fluid Mechanics*. Springer-Verlag, New York, third edition edition, 1994.
- [7] J. delA lam o and J. Jimenez. Spectra of the very large anisotropic scales in turbulent channels. *Physics of Fluids*, 15(6):L41, 2003.
- [8] M. Germano, U. Piomelli, P. Moin, and W.H. Cabot. A dynamic subgrid scale eddy viscosity model. *Phys. Fluids A*, 3(7):1760{1765, 1991.
- [9] S. Ghosal, T.S. Lund, P. Moin, and K. Akselvoll. A dynamic localization model for large-eddy simulation of turbulent flows. *J. Fluid Mech*, 285:229{255, 1995.
- [10] D.D. Holm. Fluctuation effects on 3D Lagrangian mean and Eulerian mean fluid motion. *Physica D*, 133:215{269, 1999.
- [11] D.D. Holm, J.E. Marsden, and T.S. Ratiu. Euler-poincare equations in geophysical fluid dynamics. In *The Mathematics of Atmosphere and Ocean Dynamics*. Isaac Newton Institute, 1998.
- [12] D.D. Holm, J.E. Marsden, and T.S. Ratiu. Euler-Poincare models of ideal fluids with nonlinear dispersion. *Phys. Rev. Lett.*, 349:4173{4177, 1998.

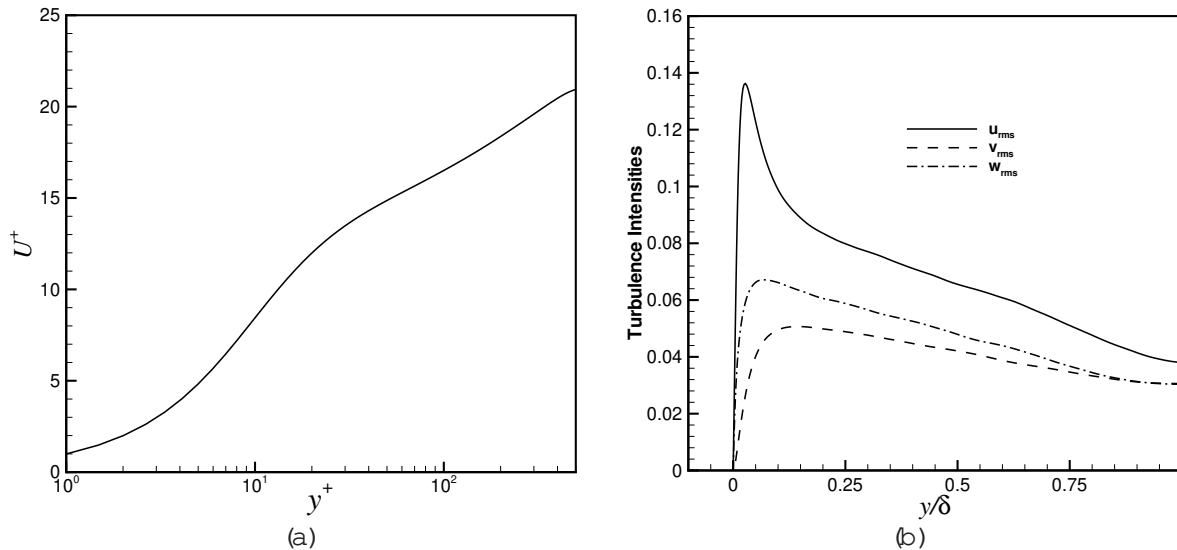


Figure 8: DNS results of a turbulent channel flow at $Re = 550$ from delAlamo and Jimenez [7]. (a) The mean velocity profile, (b) Root-mean-square velocity fluctuations in global coordinates.

- [13] H.G. Im, T.S. Lund, and J.H. Ferziger. Large eddy simulation of turbulent front propagation with dynamic subgrid models. *Phys. Fluids*, 9:3826{3833, 1997.
- [14] C. Kane, J.E. Marsden, M. Ortiz, and M. West. Integrators and the newmark algorithm for conservative and dissipative mechanical systems. *Int. J. Num. Math. Eng.*, 49:1295{1325, 2000.
- [15] J. Kim, P. Moin, and R. Moser. Turbulence statistics in fully developed channel flow at low Reynolds number. *J. Fluid Mech*, 177:133{166, 1987.
- [16] A. Lew, J.E. Marsden, M. Ortiz, and M. West. A synchronous variational integrators. *Archive for Rat. Mech. Anal*, 167 (2):85{146, 2003.
- [17] D.K. Lilly. A proposed modification of the Germano subgrid-scale closure method. *Phys. Fluids*, 4:633{635, 1992.
- [18] J.E. Marsden and T. Ratiu. *Introduction to Mechanics and Symmetry*. Springer-Verlag, New York, second edition edition, 1998.
- [19] J.E. Marsden and S. Shkoller. The anisotropic lagrangian averaged euler and navier-stokes equations. *Arch. Rational Mech. Anal*, 166 (27-46):27{46, 2002.
- [20] C. Meneveau and T.S. Lund. The dynamic Smagorinsky model and scale-dependent coefficients in the viscous range of turbulence. *Phys. Fluids*, 9 (12):3932{3934, 1997.
- [21] K. Mohseni. Statistical equilibrium theory of axisymmetric flows: Kelvin's variational principle and an explanation for the vortex ring pinch-off process. *Phys. Fluids*, 13 (7):1924{1931, 2001.

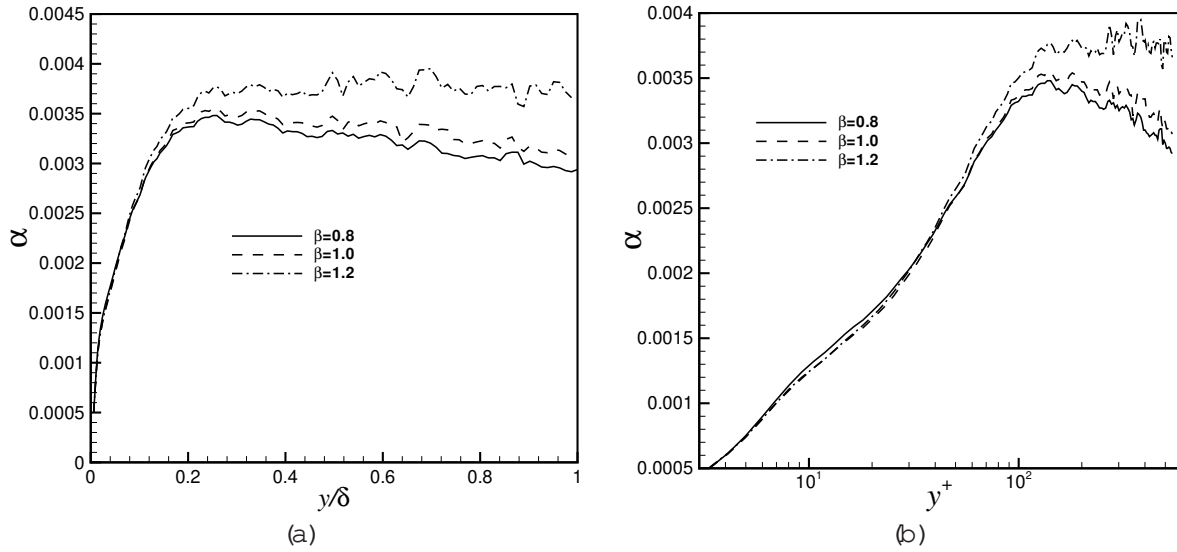


Figure 9: Variation of α with distance from the wall in (a) global, and (b) wall units.

- [22] K. M. Mohseni, B. Kosovic, S. Shkoller, and J. E. Marsden. Numerical simulations of the Lagrangian averaged Navier-Stokes (LANS-) equations for homogeneous isotropic turbulence. *Phys. Fluids*, 15(2):524{544, 2003.
- [23] R. D. Moser, J. Kim, and N. N. Mansour. Direct numerical simulation of turbulent flow up to $Re = 590$. *Phys. Fluids*, 11(4):943{945, 1999.
- [24] D. C. Wilcox. *Turbulence modeling for CFD*. DCW Industries, La Canada, CA, 1993.

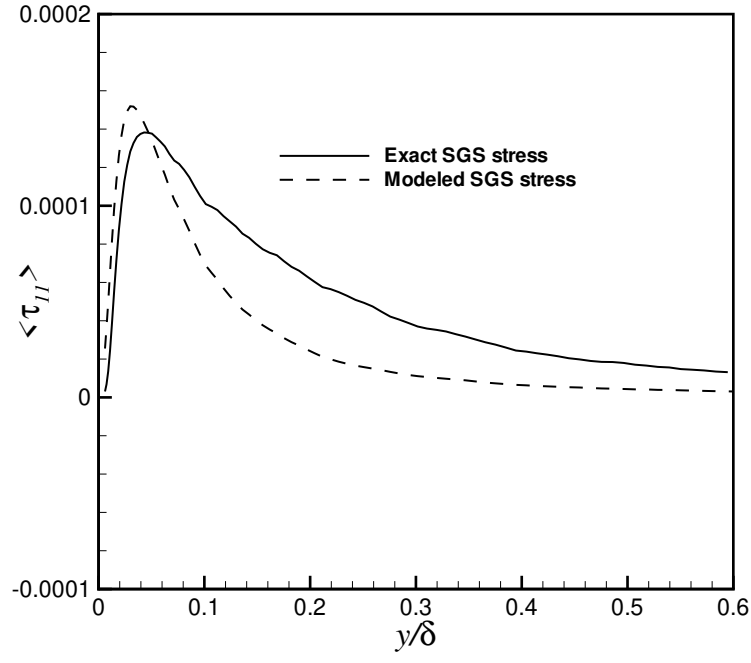


Figure 10: The averaged subgrid scale normal stress $\langle \tau_{11} \rangle$ in global units.

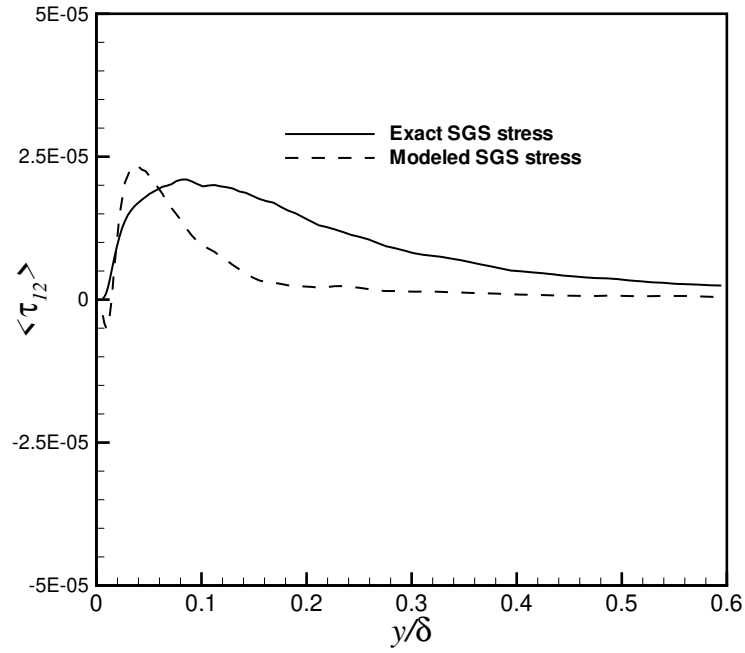


Figure 11: The averaged subgrid scale shear stress $\langle \tau_{12} \rangle$ in global units.

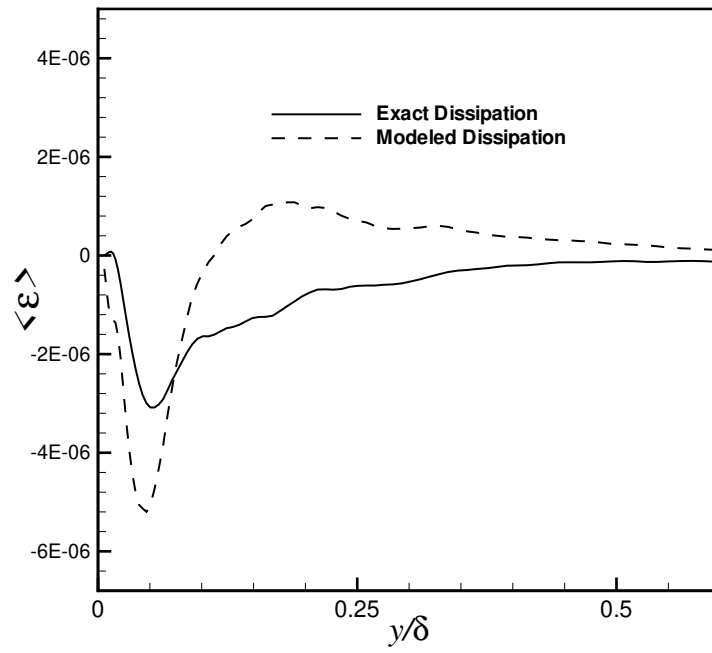


Figure 12: The averaged dissipation in global units.